Absence of magnetic state dependent low-frequency noise in spin-valve systems

Feng Guo, Greg McKusky, and E. Dan Dahlberg

Phys. Rev. B **88**, 014409 — Published 9 July 2013

DOI: 10.1103/PhysRevB.88.014409

Absence of magnetic state dependent low frequency noise in spin valve systems

Feng Guo*, Greg McKusky and E. Dan Dahlberg+

School of Physics and Astronomy, University of Minnesota, Minneapolis, MN 55455

Abstract

The low frequency noise in magnetic tunnel junctions and giant magnetoresistance devices in various magnetic states has been investigated. The noise measurements in both types of devices show a 1/f spectrum in either the parallel or antiparallel magnetic state. The noise as the magnetization switches from parallel to antiparallel and *vice versa* in the transition regions, characterized by a large dR/dH, also exhibits a 1/f spectrum of a magnitude consistent with that in the parallel and antiparallel states. This is different from many previous measurements. Included is how even small magnetic aftereffect signals can replicate the results of many previous studies. Two additional experiments are described which set an upper limit for the magnetic noise in the devices investigated.

Index Terms- Magnetic Tunnel Junctions (MTJ), 1/f noise, Giant Magnetoresistance (GMR)

PACS numbers: 75.60.Ej, 75.60.Lr, 85.75.-d, 75.75.-c

* guo@physics.umn.edu

+ dand@umn.edu

I. INTRODUCTION

Since the discovery of giant magnetoresistance (GMR) [1, 2] and the development of magnetic tunnel junctions (MTJ) [3, 4], spintronics has progressed rapidly. As a result of the new physics and the development of applications such as hard drive read head sensors and other magnetic field sensors, both MTJ and GMR systems have been extensively studied [5]. In the case of disk drive read heads and magnetic field sensors the need to minimize the noise is important while at the same time understanding the noise provides a window to various physical processes in magnetic materials. In the case of MTJs there have been a number of studies that focus on the noise [6-13]. In most of these [6-12] is reported a significant increase in the low frequency (1/f) noise when dR/dH is large which occurs when a magnetic layer is reversing which is attributed to magnetic fluctuations. In two of these [12, 13] is reported a large change in the spectral exponent of the noise when dR/dH is large, again attributed to magnetic fluctuations. It is important note two of these previous works use devices that are smaller than the smallest reported here [6.8] and in those features of random telegraph noise (RTN) are observed which may indicate switching between two equivalent magnetic states in one of the layers. Thus previous research on the noise in MTJs reports an increase in the magnitude of the magnetic noise at low frequency, i.e. 1Hz, by a factor of 10 to 100 when dR/dH is large and the two that characterize the noise as $1/f^{\alpha}$ found that α increases from 1 to about 2 when dR/dH is large.

In order to better understand these results, we have focused on the origin of the reported low frequency noise and its correlation with the magnetic state. We have measured the time dependence of the resistances of the devices and the noise spectra in various magnetic states and, as an extension of our previous work on MTJs [15], include similar studies on GMR devices.

Our results can be summarized in two statements. First, we always observed a magnetic aftereffect or magnetic viscosity [16] (a slow relaxation of the magnetic state) when dR/dH was large. Second, we found the presence of a magnetic aftereffect during a noise measurement can replicate both the increase in the magnitude of low frequency noise and the increase in α to values larger than 1 observed by others.

Our results presented here are in disagreement with the previously published work because when accounting for the magnetic aftereffect we always find the 1/f noise present to have a similar magnitude for all magnetic states (for all values of dR/dH from large to zero) and applied fields. Regarding this disagreement, we note that our devices have dimensions of either 300 μm×300μm or 10μm×10μm for the MTJ devices and 1.8mm×9.0mm for the GMR devices, a point we will address further in the conclusions with regards to the work on smaller devices [6,8].

The results of our studies clearly indicate caution must be taken to assure that measured magnetic noise spectra are the result of stationary noise and not an artifact due to the magnetic aftereffect. Although we can replicate the previously published noise results with an artifact due to the magnetic aftereffect, we do not conclude those measurements are in error as sufficient detail of the experimental procedures are not presented in those works and some of the previous work is on devices smaller than ours reported here.

In addition to the above, other new studies included here are: 1) a simple calculation to show analytically how the magnetic aftereffect can give rise to an apparent increase in low frequency noise and a qualitative demonstration of this; 2) a quantitative discussion of how the magnitude of a magnetic aftereffect alters noise measurements; 3) two experiments which set an upper limit of low frequency magnetic noise in our devices when dR/dH is not large.

In the following we first describe the sample fabrication as well as the experimental procedures. This is followed by the low frequency noise data and studies of the time evolution of the devices' resistances when one of the magnetic layers is switching. The time evolution experiments clearly indicate the presence of a magnetic aftereffect in the devices when a magnetic layer is switching. A study of the time dependence of the noise spectra (repeated measurements of the noise) in our devices after a target magnetic field is reached directly shows how the magnetic aftereffect can give rise to a measured increase in the low frequency noise and can increase the frequency dependence of this noise from 1/f to 1/ f^2 depending upon the amount of magnetic aftereffect present. We next show with a simple calculation how the magnetic aftereffect and 1/f noise can be mixed in a noise measurement to mimic the reported magnetic noise. A qualitative evaluation is then made to demonstrate how the magnetic aftereffect alters the measured noise. We also describe two experiments attempting to determine magnetic contributions to the low frequency noise. One is an investigation of the noise in large magnetic fields and the other is measurements of the noise as a function of the angle between the magnetizations. We lastly summarize our work in the conclusion and compare it to the previous results.

II. SAMPLE FABRICATION AND EXPERIMENT DETAILS

The MTJ stacks were made by dc sputtering in 3 mTorr of Ar a stack consisting of $Ni_{81}Fe_{19}$ (10 nm)/ $Co_{90}Fe_{10}$ (3 nm)/ AlO_x (1.5 nm of Al before oxidation)/ $Co_{90}Fe_{10}$ (5 nm)/ FeMn (5 nm). The $Ni_{81}Fe_{19}$/ $Co_{90}Fe_{10}$ bilayer provided a magnetic soft layer with a switching field usually smaller than 30 Oe and the exchange coupled $Co_{90}Fe_{10}$/ FeMn bilayer provided a relatively large coercivity; this selection of materials enabled the MTJ devices to have a reasonably antiparallel state of the magnetizations for some value of an applied field. There were 17 tunnel junctions investigated which

were defined by shadow masks during deposition resulting in MTJ areas with dimensions on the order of 150μm×300μm; there were 8 MTJs studied which were processed by ion mill and lithographic techniques resulting in junction areas with nominal dimensions of 10μm×10μm.

The GMR samples were made by dc sputtering in 3 mTorr of Ar a stack consisting of Ta (6nm)/ $IrMn_4$ (8nm)/ $Co_{90}Fe_{10}$ (3.5nm)/ Cu (2.1nm)/ $Co_{90}Fe_{10}$ (1nm)/ $Ni_{81}Fe_{19}$ (4.5nm)/ Ta (3nm) in which the exchange coupled bilayer IrMn/CoFe formed a pinned layer with a relatively large coercive field while the CoFe/NiFe bilayer served as a relatively free layer; the 10 GMR samples we measured were rectangular in shape with dimensions of 1.8mm×9.0mm; for all these the pinned magnetization was along the long axis and was collinear with the applied field except where noted.

The transport and noise measurements were four-terminal and we are presenting here our results at ambient temperature. A battery with a current limiting resistance was used as a constant current source for both resistance and noise spectrum measurements. The sample voltages were amplified by 10^3 with a SR560 amplifier before the power spectral densities, PSD or S_v, were measured with a HP34560A spectrum analyzer. The noise data was usually averaged over multiple measurements, typically 25, and for the noise data shown the preamp gain of 10^3 has been removed (as well as for all data shown here).

The experimental equipment and procedures used in our noise measurements were checked by two methods. From a Johnson noise analysis of the noise spectra of several different resistance values of metal film resistors a value for the Boltzmann constant, k_B, was found to be $1.37\pm0.02\times10^{-23}$ J/K in agreement with the accepted value. We also measured the shot noise of a photodiode and from an analysis of that data a value for the electron charge, e, was determined to be $1.63\pm0.04\times10^{-19}$ C, again in agreement with the accepted value.

In figure 1 is a typical noise spectrum of a MTJ in the low resistance state, i.e., with the magnetizations parallel. As shown at low frequencies, below 1 kHz for example, the noise scales as 1/f

as indicated by the solid line with a slope of -1 beneath the low frequency part of the spectrum and at higher frequencies the spectrum is frequency independent and is due to a combination of thermal noise and shot noise; the upper dashed line in Fig. 1 is the calculated white noise based on the junction resistance; in this figure and all similar figures we do not subtract the intrinsic noise of the apparatus so the calculated noise includes this background. In the same figure is the noise from a metal film resistor without an applied voltage having a resistance comparable to that of the MTJ. Clearly the sample's 1/f noise is larger than the background noise but the question is if this is magnetic noise or noise from other sources such as the tunnel junction oxide. For now we simply state we can find no evidence this 1/f noise is magnetic in origin and will return to this statement later in the paper.

In both the parallel (P) and antiparallel (AP) magnetic states the spectra of the MTJ (for the MTJs it is a nominally antiparallel state as there is not a well defined resistance plateau but since the MTR ratio value is about 25% it is reasonably close to antiparallel) and GMR devices all exhibit similar behaviors. Also, in the transition regions where dR/dH is large we do not expect the magnetization to be uniform and in the smaller junctions may be an evolving S-state or C-state magnetization. The main differences between the MTJ and GMR devices is the white noise in the GMR devices is exclusively from the thermal noise.

III. DATA AND ANLYSIS

We have measured the noise of 25 MTJ samples and 10 GMR samples with various resistances and sizes, and the features discussed here have been found in all of them. For all samples measured the values of the higher frequency noise, above the 1/f regime, are consistent with the values calculated for the thermal and shot noise of the device being studied.

Representative examples of the magnetic field dependence of the measured noise are shown in Fig. 2 for both a MTJ and a GMR device; the magnetic state can be inferred from the magnetoresistance measurements in Figs. 2a and 2c for the MTJ and the GMR samples respectively. For the MTJ sample, the points A and E in the resistance curve 2a are both parallel magnetization states of the ferromagnetic layers while the point C is at a magnetic field where the electrodes are in the nominally antiparallel state; the noise measured in either the P or the AP state displays a 1/f spectrum as illustrated in Fig 2b by the plots labeled A and C (the solid lines in these two figures are 1/f). The value of dR/dH is large when the MTJ is switching from the P to AP states or *vice versa*, such as points B and D in Fig 2a, and the measured spectrum is found to be $1/f^2$ as shown in the plot labeled B in Fig. 2b (the line in this figure is $1/f^2$). It is important to note these spectra were taken as soon as the target magnetic field was reached and thus include the effects of the magnetic aftereffect as we discuss later. One should notice that the magnitude of the noise at 1 Hz in plot B is over a factor of 100 times larger than the 1 Hz noise in plots A and C in Fig. 2b.

Similar data are plotted for the GMR device in Fig. 2c and 2d. The points labeled F and J are in parallel (P) magnetization states while the point labeled H is in an antiparallel (AP) state; both of the P and AP states yield 1/f spectra as shown in Fig. 2d where the noise spectra for points F and H are plotted. As in the MTJ, the GMR device in the transition regions illustrated by points G and I exhibit a measured noise spectrum which is $1/f^2$ and also has a similar increase in the magnitude of the frequency dependent noise as shown the spectrum measured at point G presented in Fig. 2d.

In order to illustrate the magnetic state dependent data, we plotted the PSD at 1Hz (normalized by V_{bias}^2) and the exponent, α, obtained by fitting the spectra with $1/f^{\alpha}$ as a function of the magnetic field in Fig. 3; again these data are from spectra taken as soon as the target magnetic field was reached. These two quantities, the low frequency noise level and the slope of the spectrum in the log-log plot,

are used to characterize the noise spectra measured in various magnetic states. Like the previous noise studies [6-13], the unexpected PSD behaviors are observed in the transition regions when either the free layer or hard/pinned layer is in the process of switching. As can be seen, in these regions the PSD at 1 Hz can be over 1000 times larger for the MTJ sample and approximately 100 times larger for the GMR sample compared to the noise in either the P or the AP states. In addition to the increase in the noise level, the exponent α increases from the usual value of 1 to values as large as 2.

To understand the apparent increase of the measured noise and the change in the noise exponent described above, we have measured the time dependent voltages with a constant current applied to both MTJ and GMR devices at various magnetic fields. The procedure we followed began with the application of a magnetic field in the positive direction to saturate the magnetizations so that a sample started in a parallel magnetic configuration. The magnetic field was then swept in the negative direction until the desired field value was reached and then measurements of the time dependence of the resistance (or voltage) were started. The usual time for data collection was about 100 seconds [17]. As the results of these measurements were qualitatively the same for all the samples of both the MTJ and GMR device structures measured we show a single illustrative example in Figure 4 for a MTJ. This figure shows the time dependent voltage of a MTJ in the P and AP states and in the applied magnetic regions when the soft or free layer is in transition and the same for the hard layer. In both the P and the AP states as seen in Figs. 4a and 4c respectively, the average voltage is time independent. At the fields corresponding to the transition regions, however, we observe significant time dependent signals in addition to the noise in the P or AP states, as shown in Figs. 4b and 4d; this large time dependence is attributed to the magnetic aftereffect or magnetic viscosity [16, 18]. Usually the magnetic aftereffect has a quasilogarithmic time dependent magnetization which we show in the inset of Fig. 4b where a plot of the logarithmic time dependence of the voltage taken as a measure of the

magnetization is presented. One should note the variation of the voltage within the 100 second measurement time due to the magnetic aftereffect is significantly larger than the peak to peak voltage noise in either the P or the AP state.

What we show next is how the presence of the magnetic aftereffect in our devices explains the observed low frequency noise increase and the deviations from 1/f behavior, i.e., they are both artifacts of the magnetic aftereffect and not a true measure of magnetic noise. To accomplish this we measured the noise spectra repeatedly over a long time period. Thus the amount of change in the signal associated with the magnetic aftereffect becomes smaller with each subsequent noise measurement and thus its contribution to the measured spectra is reduced with time. In essence, measuring the spectrum repeatedly at a specific field value has the same effect as reducing the magnetic aftereffect.

The procedure we followed for this study is similar to what was described before. First the magnetizations were saturated in a large positive magnetic field and then the field was swept in the negative direction until the switching region of one of the films' magnetization was reached such as points D and B in Fig. 2a and points I and G in Fig. 2c. Upon reaching a field value that falls in the transition region, the magnetic field was held constant while the spectrum was measured repeatedly over a period of time. With this process we had a number of spectra taken at various times after the target magnetic field was reached and thus the time evolution of the spectra was obtained. The PSD at 1Hz and α are obtained from each measured spectrum and the time evolution of the two is plotted. Examples of the results of these studies are presented in Figs. 5a and 5b for a MTJ and a GMR sample respectively as the soft layer is switching such as points B and I in Figs. 2a and 2c. As shown the spectra for both devices begin with a large low frequency noise level as illustrated by the 1 Hz noise magnitude and a large value of α like the noise data in the transition regions in Fig. 3. Over the 400 sec in the case of the MTJ, however, the PSD at 1Hz gradually decays and approaches a value that is

consistent with the noise level in the P and AP states and simultaneously the value of α decreases from 2 to a value of 1.

The above measurements clearly indicate the logarithmic variation of the device voltage is altering the measured spectra, even without the presence of Barkhausen jumps. (Note: The Barkhausen jumps would diminish with time and thus, by definition, cannot be considered as stationary noise.)

Further proof that both the increase in magnitude of the low frequency noise and the deviations from 1/f behavior can be artifacts of the magnetic aftereffect comes from mathematically generating an artificial signal which consists of 1/f noise and a logarithmic time dependent function and then determining the PSD of this combination. In more detail, we generated a time dependent signal having a pure 1/f spectrum with the 1Hz component set to a value of 3×10^{-15} V^2/Hz which is comparable to the measured noise level for our MTJ devices. This 1/f noise was then added to a function replicating the magnetic aftereffect which was a logarithmic function of the form $A_{AE}\,\mathrm{Log}(t+0.1)$ with the magnitude of the prefactor, A_{AE}, determining the amount of magnetic aftereffect present. In other words if A_{AE} =0 then there is no magnetic aftereffect just like the P and the AP states and any nonzero values of A_{AE} indicate the presence of some magnetic aftereffect. The PSDs of these simulated time signals were determined for various values of A_{AE}, with the results of the magnitude of both the PSD at 1Hz and α as functions of A_{AE} plotted in Fig. 6a. As one can see from this figure as A_{AE} is increased, equivalent to increasing the magnetic aftereffect present during a measurement, the spectra evolve from 1/f to approximately $1/f^2$ while the magnitude of the 1 Hz noise also increases by a factor of about 1000 for the values of A_{AE} used; the saturation of α to a value close to 2 can be shown analytically as mentioned in the next paragraph. A parametric plot to illustrate the correlated change of α and the 1Hz PSD with increasing A_{AE} is shown in Fig. 6b. To compare this with actual noise data, Figs. 6c and 6d show the

correlation between α and the 1 Hz component of the spectra presented in Fig. 3 for the MTJ and the GMR device respectively.

One can also show how the logarithmic function can alter the measured spectra in a more analytical fashion, i.e., calculating the PSD of the logarithmic function, $A_{AE}\,\mathrm{Log}(t+t_0)$. This can be accomplished by taking the Laplace transform with the time domain variable *t* being transformed to a complex variable *a* + *iw* and then taking the limit as *a* goes to zero. When this is done, one finds PSD's of the form $1/f^{\alpha}$ with α close to 2 for t_0 on the order of 0.1 sec and the magnitude of the PSD determined by A_{AE}. One can also numerically take the FFT of a logarithm, square it and plot the resultant function to again find a similar result. Thus both these approaches explain the saturation of α seen in Fig. 6b.

The next obvious question to ask is how large a change in voltage across a device during a measurement period due to the magnetic aftereffect, i.e, a logarithmic time dependence, would distort the measurements. The magnitude of the magnetic relaxation may vary in different devices as it is determined by many factors including the choice of material, magnetic state and history, device size, temperature, etc. Despite the variation, we now discuss the general case that applies to all the devices. In particular how the alteration of the measured PSD due to the aftereffect depends on the rate of the voltage drift.

Consider the situation where the magnetic aftereffect causes a voltage change of δV during the measurement period of 1 second in this example, i.e., after the application of the target magnetic field the voltage across the device evolves logarithmically with time due to the magnetic aftereffect. To understand how this δV affects the measurements, we calculated the PSD one would obtain as a function of δV. This calculation included only the logarithmic function without any intrinsic 1/f component. In figure 7a we show the magnitude of the PSD at 1 Hz, which we call S_v^{Log}, scales as

$(\delta V)^2$. This clearly shows the remarkable sensitivity of noise measurements to the presence of any magnetic aftereffect, as demonstrated in figure 7b. The inset in figure 7a are the PSDs calculated for several values of δV; the slope of the PSDs, α, is somewhat less than 2.

Since the PSD associated with the magnetic aftereffect and the actual noise in a device are uncorrelated, their combined effect on the spectral power would be additive. Thus a determination for how large a magnetic aftereffect voltage change during a measurement time, δV, is best illustrated by considering the ratio of the value of the total PSD at 1 Hz from both the magnetic aftereffect and the actual noise of one of our typical devices to the value of the PSD at 1 Hz in one of our typical devices without the presence of any magnetic aftereffect. This ratio is shown plotted in figure 7b as a function of both δV (upper X-axis) and as a percentage of the device bias voltage (lower X-axis) which is about 50mV in this case. As can be seen in this figure, extreme care must be taken in assuring the device being measured is close to equilibrium as even a small voltage drift due to the magnetic aftereffect associated voltage can drastically alter the measurement results. For example, a small voltage drift with a $\delta V/V_{bias}$ ratio of 1.6×10^{-3} increases the total PSD with respect to the original PSD by about a factor of ten.

So far, we have shown we have an alternate explanation of the origin of the previously reported unexpected noise in transition regions but this raises a separate question. We now ask if there any 1/f or low frequency noise for our MTJ or GMR devices that is clearly associated with the magnetism?

Two experiments were designed to address this question. We first note that for the field ranges shown so far, the magnetization may not be uniform nor completely aligned to the applied field even in the P-state; the first experiment addresses this issue. A variable magnetic field was applied in-plane to a MTJ with the magnetizations parallel to the field direction. The field was varied from about 100 Oe up to 2×10^4 Oe. At a number of fixed magnetic fields the MTJ voltage and the noise spectrum were

recorded. The results of this are shown in Fig. 8 where in Fig. 8a the MTJ voltage (proportional to the resistance) is shown and the noise magnitude at 1 Hz is shown in Fig. 8b. The 2% drop in voltage implies the increasing field forces the magnetizations to be more aligned while there is no measurable change in the 1 Hz PSD. Although there is no apparent change in the low frequency noise in this measurement this null result is certainly not conclusive given the small voltage (resistance) change and the scatter in the 1 Hz noise component.

The second investigation consisted of measuring the noise spectrum as a function of angle between the two magnetizations in a GMR device. An applied magnetic field of 100 Oe was chosen such that it is was well below the switching field of the pinned layer but higher than the switching field of the free layer. By rotating the magnetic field in the plane of the sample the free layer followed the applied field thereby changing the angle between the magnetizations. The resistance of the GMR device and the noise spectrum were measured as a function of the angle between the two magnetizations. The results of this are shown in Fig. 9 where the angular dependence of the device resistance (Fig. 9a) and the magnitude of the 1 Hz noise (Fig. 9b) are plotted. The resistance versus angle data are consistent with the angular dependence expected for a GMR device [19] with the P state (0 degree, 360 degrees) having a low resistance and the AP state (180 degrees) having the highest resistance. The noise spectrum was also measured at various angles and was averaged over 100 measurements. The 1Hz component of the PSD as a function of angle is shown in Fig. 9b and no significant angular dependence of noise within the measurement error is observed in the data. Again, although we do not observe any noise in our measured samples which we can attribute to magnetic fluctuations this null result merely sets an upper limit for the magnetic noise.

III. CONCLUSIONS

In summary, when care is taken to remove possible artifacts in measured noise spectra due to the magnetic aftereffect, we do not observe any measureable differences in the noise spectra between the P state, AP state and the transition regions when dR/dH is large other than those expected due to differences in the state dependent resistance. To summarize our observations of the stationary noise in MTJs and GMR devices, in the P and the AP states and in the transition regions when dR/dH is large the low frequency spectrum is always 1/f and consistent with the absence of observable magnetic noise.

One possible explanation for the difference in the results presented here and those of others is we have observed in the magnetic transition regions (P to AP and AP to P transitions) when dR/dH is large the slow quasi-logarithmic time dependent relaxation known as the magnetic aftereffect was always present. In our measurements when the magnetic aftereffect was experimentally accounted for there was no observation of magnetic noise; if the effects of the magnetic aftereffect were included in the data accumulation the noise measurements indicated PSD spectra of the form $1/f^{\alpha}$ with α between 1 and 2 and a significant related increase in the low frequency PSD magnitude. A causal relationship between both the magnitude of the measured low frequency noise and the PSD spectra exponent and the time evolution caused by the aftereffect was determined in two ways.

The first consisted of measuring the time dependence of the spectrum in the large dR/dH transition regions. We found the measured spectrum started as a $1/f^2$ spectrum and then evolved to that of 1/f noise while the 1Hz component of the PSD diminished to its normal level of that in the P and AP states in this relaxation process.

The second method extends our observations to the more general case for any device with magnetic relaxation present. It consists of calculating the PSD of the sum of a 1/f signal and a logarithmic time dependent function. We found as the component of the logarithmic signals increase,

as would describe the magnetic transition states, the apparent spectrum evolves to the $1/f^2$ type and there was an associated increase in the low frequency noise level. We also pointed out briefly that this is consistent with the analytically determined PSD for a logarithmic function of time.

These two independent methods directly support our conclusions that for all the samples we have measured the magnetic aftereffect is responsible for the observations of increased noise in the transition regions similar to those described in a number of reports [6-12, 14] and the increase in the spectral exponent of the noise from 1 to 2 in other reports [12, 13]. We conclude that the magnetic relaxation in the measured devices will distort the apparent low frequency noise level and thus it is clear that care needs to be taken to avoid the possible artifact when measuring noise spectra in magnetic systems when a possible magnetic aftereffect is present.

It is a certainty that magnetic noise exists, however, the observation of magnetic noise requires it to be significant compared to other noise present, such as Johnson or shot white noise or 1/f noise; this sets the lower limit on the necessary magnitude of the magnetic fluctuations which was part of the motivation for two of the experiments described at the end of this paper. These two experiments do not address our lack of observation of any magnetic noise or magnetic fluctuations in our devices when dR/dH was large. As pertains to when we are in a regime of large dR/dH in our samples, we will briefly consider two cases, a "macroscopic" magnetic film and a "microscopic" magnet.

We define the macroscopic magnetic film as a thin film with planar dimensions on the order of a few tens of microns which describes both magnetic layers of our shadow mask manufactured MTJs and GMR devices and one layer of the lithographically prepared MTJs. In this limit, when the magnetization change with applied field, dM/dH, is large the magnetic reversal most likely consists of domain wall propagation; this is consistent with the Barkhausen jumps we observed. In the literature

w e are unable to find reports of Barkhausen jumps in both directions during reversal, i.e., once a wall moves to a lower energy state it does not reverse.

In the microscopic limit, which for our smallest devices (MTJs with dimensions of 10μm×10μm) may not be sufficiently small enough to be considered microscopic, significant fluctuations may occur when dM/dH is large when are there magnetic states which are closely related in energy separated by an energy barrier on the order of k_BT; clearly in our samples we do not observe these type of fluctuations. Expanding on the importance of sample size, two of the studies utilized devices significantly smaller than those studied here. In particular the work by Ingvarsson and co-workers, [8] measured samples with an area of 0.45 μm^2, and 2 μm^2 and the work by Jiang and co-workers, [6] worked in part on junctions with areas down to 0.4 μm^2 which are significantly less than our smallest sample investigated with an area of 100 μm^2. Both of these studies presented results which indicate the presence of RTN but did not fully investigate the origin. Given the small areas and the observation of RTN features in their data suggest the possibility of magnetic states which are closely related in energy separated by an energy barrier on the order of k_BT. Certainly the presence of fluctuations leading to RTN depends upon the size, shape, and magnetic properties of the elements and, although of significant importance, this issue remains mostly unexplored although there are recent efforts in this area [20, 21].

We would like to acknowledge useful conversations with Professor Randall Victora, a helpful suggestion from Jin Chen on the analytical solution of the Fourier transform of the logarithm, Peter Dahlberg for the numerical PSD of a logarithm. This work was supported by the MRSEC Program of the National Science Foundation under Award Numbers DMR-0212302 and DMR-0819885 and by the Office of Naval Research under Award Number N00014-11-1-0850. Parts of this work were carried

out in the Institute of Technology Characterization Facility, University of Minnesota, which receives partialsupport from NSF through the NNIN program.

References:

[1] M. N. Baibich, J. M. Broto, A. Fert, F. Nguyen Van Dau, F. Petroff, P. Etienne, G. Creuzet, A. Friederich, and J. Chazelas, Phys. Rev. Lett. 61, 2472 (1988)

[2] G. Binasch, P. Grunberg, F. Saurenbach, and W. Zinn, Phys. Rev. B 39, 4828 (1989)

[3] M. Julliere, Phys. Lett. 54 (1975) 225

[4] J. S. Moodera, L. R. Kinder, T. M. Wong, and R. Meservey, Phys. Rev. Lett. 74, 3273, (1995).

[5] E. Y. Tsymbal, O. N. Mryasov, and P. R. LeClair, J. Phys: Condens. Matter 15 (2003) R109-R142; J. S. Moodera and G. Mathon, J. Magn. Magn. Mater. 200 (1999) 248; J. S. Moodera, J. Nassar and G. Mathon, Annu. Rev. Mater. Sci. 1999. 29: 381-432; S. S. P. Parkin, Annu. Rev. Mater. Sci. 1995, 25: 357; E.Y.Tsymbal and D.G.Pettifor, Solid State Physics, 56, 113 (2001)

[6] L. Jiang, E. R. Nowak, P. E. Scott, J. Johnson, J. M. Slaughter, J. J. Sun, and R. W. Dave, Phys. Rev. B. 69, 054407 (2004).

[7] C. Ren, X. Liu, B. D. Schrag, and G. Xiao, Phys. Rev. B. 69, 104405 (2004).

[8] S. Ingvarsson, G. Xiao, S. S. P. Parkin, W. J. Gallagher, G. Grinstein, and R. H. Koch, Phys. Rev. Lett. 85, 3289 (2000).

[9] D. Mazumdar, X. Liu, B. D. Schrag, M. Carter, W. Shen, and G. Xiao, Appl. Phys. Lett. 91, 033507 (2007).

[10] D. Mazumdar, X. Liu, B. D. Schrag, W. Shen, M. Carter and G. Xiao, J. Appl. Phys. 101, 09B502 (2007).

[11] D. Mazumdar, W. Shen, X. Liu, B. D. Schrag, M. Carter and G. Xiao, J. Appl. Phys. 103, 113911 (2008).

[12] A. F. Md Nor, T. Kato, S. J. Ahn, T. Daibou, K. Ono, M. Oogane, Y. Ando, and T. Miyazaki, J. Appl. Phys. 99, 08T306 (2006).

[13] R. Guerrero, F. G. Aliev, R. Villar, R. Ortega-Hertogs, W. K. Park, and J. S. Moodera, J. Phys. D. 35, 1761 (2002).

[14] R. J. M. van de Veerdonka, P. J. L. Belie¨nb, K. M. Schep, J. C. S. Kools, M. C. de Nooijer, M. A. M. Gijs, R. Coehoorn and W. J. M. de Jonge, J. Appl. Phys. 82, 6152 (1997).

[15] F. Guo, G. McKusky, and E. D. Dahlberg, Appl. Phys. Lett. 95, 062512 (2009).

[16] J. L. Snoek, Physica (Amsterdam) 5, 663 (1938). See Physics of Magnetism by S. Chikazumi and S. H. Charap, (Robert E. Krieger, Malabar, FL, 1964), chapter 15.

[17] In this experiment, the time when the magnetic field reaches the field of interest is defined as t=0.

[18] In figure 4d Barkhausen jumps are observed. These jumps are generally observed in our junctions with the switching of the hard layer. These observed discrete jumps coexist with the logarithmic evolution of time.

[19] L. B. Steren, A. Barthélémy, J. L. Duvail, A. Fert, R. Morel, F. Petroff, P. Holody, R. Loloee, and P. A. Schroeder, Phys. Rev. B 51, 292 (1995).

[20] J.F. Feng, Z. Diao, Gen Feng, E.R. Nowak, and J.M.D. Coey, Appl. Phys. Lett. 96, 052504 (2010).

[21] Daniel Endean, C. T. Weigelt, R. H. Victora, E. Dan Dahlberg, submitted for publication.

Figure Captions

Figure 1. (a) A typical noise spectrum (upper curve – black data) for a MTJ with a junction resistance of about 270Ω in the parallel magnetization configuration with 80mV applied; the noise spectrum of a 274 Ω metal film resistor (lower curve- red data) is also shown. The data are the raw data, i.e., the background noise of the experimental equipment ($S_V^{background}$@1Hz = 1.6×10^{-15} V^2/Hz and above 1 kHz $S_V^{background}$ = 1.6×10^{-17} V^2/Hz) was not subtracted. The solid line beneath the MTJ spectrum has a slope of -1, indicating the 1/f nature of the spectrum at lower frequencies; the upper horizontal dashed line (red) that matches the high frequency region of the MTJ noise spectrum is the calculated noise level which includes both Johnson and shot noise; the lower line (blue) shows the calculated thermal noise level for the metal film resistor including the background. Figures (b) and (c) show the bias dependence of the 1Hz S_V for a MTJ and a GMR sample, respectively, measured in the P-state. The solid lines in (b) and (c) indicate a V^2 dependence.

Figure 2. The plots (a) and (c) are the dc resistance of the MTJ and GMR samples respectively with the magnetic field swept from positive to negative values. When measuring the spectra, a 50mV and 160mV bias voltage are applied to the MTJ and GMR samples respectively. The three plots in (b) are PSDs of the MTJ sample taken at the points A, B, and C marked in the resistance curve. The PSD taken at the point marked E is similar to that taken at point A, and B is similar to D. In plots labeled A and C in (b) the solid lines are 1/f and in B it is$1/f^2$. Shown in (d) are the same noise measurements for the GMR sample and similar features are observed; the spectra in the parallel states, points F and J, and antiparallel state, point H, have 1/f noise. During the magnetization reversal, such as points G and I, the PSD scales as $1/f^2$ as illustrated by the line under the data in the spectrum labeled G. Artifacts of the magnetic aftereffect are included in the spectra taken at points B and G.

Figure 3. Two parameters, the PSD at 1Hz (normalized by the square of DC bias voltage) and the spectral exponent α, used to characterize the measured noise spectra are shown for a MTJ and a GMR device. The MTJ PSD magnitude as a function of the magnetic field is shown in (a); and α fitted from the low frequency part of the spectrum is plotted in (b). The GMR PSD magnitude is

in (c) and α is in (d). The field dependent resistance of the two devices are included in (a) and (c). The PSD data and α are the square and circular data respectively.

Figure 4. Shown is the time dependence of the voltage of a MTJ starting when a target magnetic field is reached; similar data were obtained for all devices measured. The data in (a) are taken in the P state such as point A in Fig. 2, those in (b) are taken in the P to AP region (soft layer switch) such as point B in Fig. 2. The data in (c) correspond to the MTJ in an AP state such as point C in Fig. 2, and the data in (d) correspond to the AP to P region (hard layer switch) similar to point D in Fig. 2. Note that (b) and (d) have larger vertical scales. The inset in (b) is the P to AP data plotted using a logarithmic scale for the time as is usually done for the magnetic aftereffect.

Figure 5. The fitted value of the exponent α (diamonds) and the magnitude of the PSD at 1Hz (squares) of a MTJ (a) and a GMR device (b) as functions of time at a constant field in the P to AP transition region of each.

Figure 6. (a) For the spectra calculated from the simulated total time signals, the value of the 1Hz PSD and the value of α are plotted as functions of A_{AE}, which determines the magnitude of the magnetic aftereffect; (b) shows the correlation between α and the PSD at 1Hz; (d) and (e) are the data from Fig. 3 for the MTJ and GMR samples respectively as a comparison.

Figure 7. (a) The 1Hz component of the PSD calculated for a pure logarithmic function as a function of δV, where δV is the change of the dc voltage on the device during the measurement time (taken as 1 sec. in this example); the straight line with a slope of 2 shows the $(\delta V)^2$ dependence of the 1Hz PSD;. The inset shows three PSDs of the pure logarithmic function with different values of δV. In (b), we plot the ratio of the 1Hz component of the total PSD (both the 1/f signal and the logarithmic function) to the value of the 1 Hz component of the 1/f PSD (taken as $3\times10^{-15}V^2/Hz$ for a typical MTJ) as functions of δV (top X-axis) and δV as the percentage of a typical dc bias voltage of 50mV (bottom X-axis).

Figure 8. (a) Voltage of a MTJ versus magnetic field for a constant applied current; (b) the 1Hz value of the measured PSD as a function of magnetic field.

Figure 9. (a) The GMR resistance as a function of the angle between the magnetizations in the two layers; (b) the angular dependence of the PSD at 1 Hz.

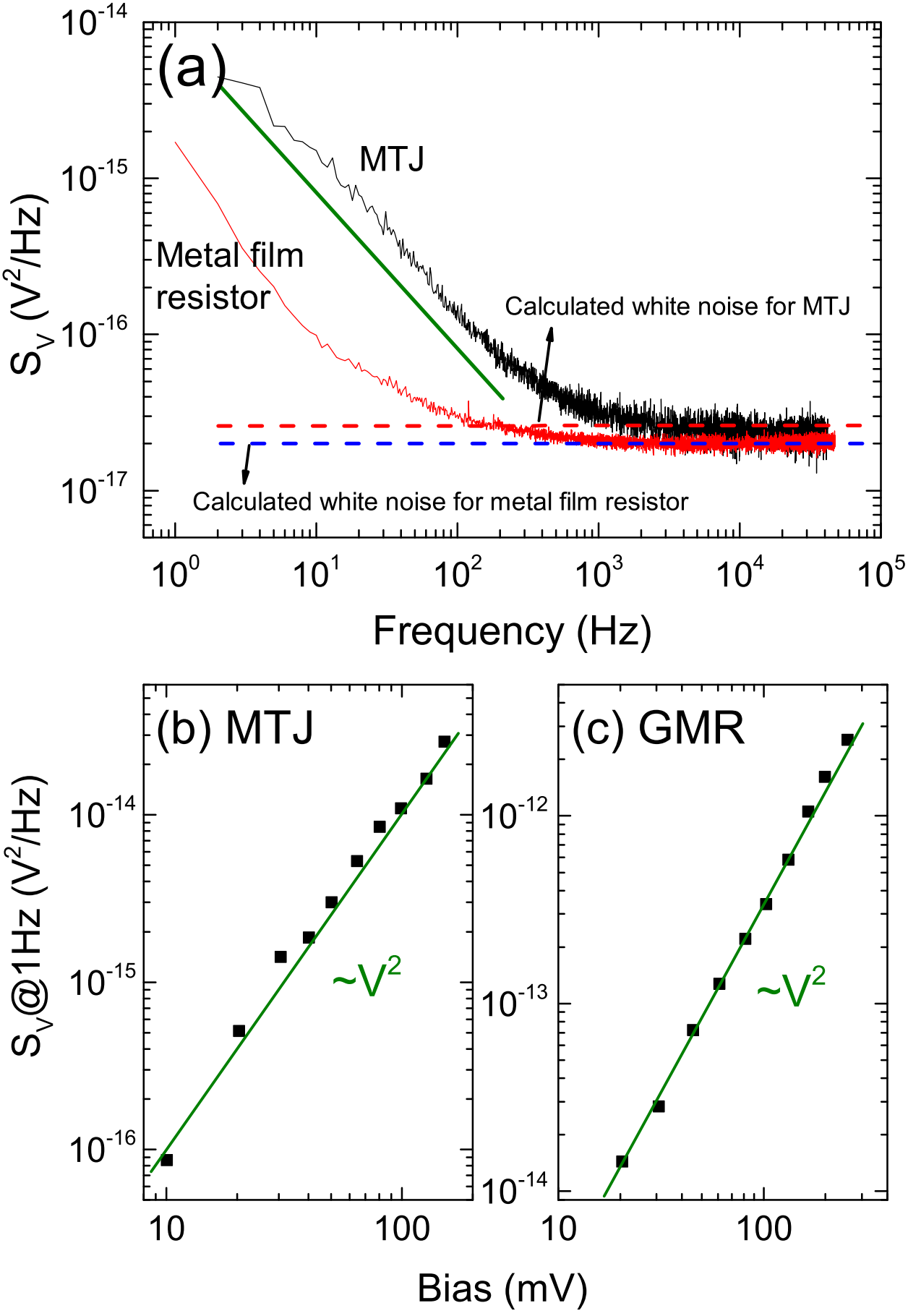

Figure 1 BP11179 28MAY2013

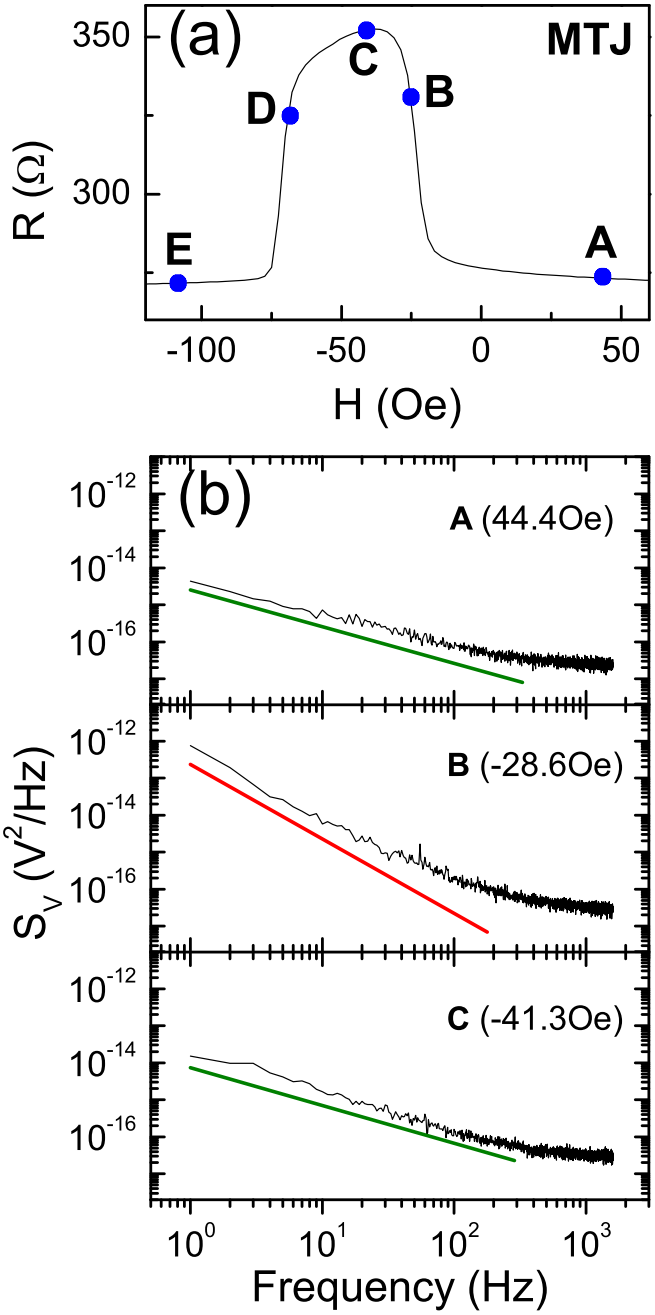

Figure 2 BP11179 28MAY2013

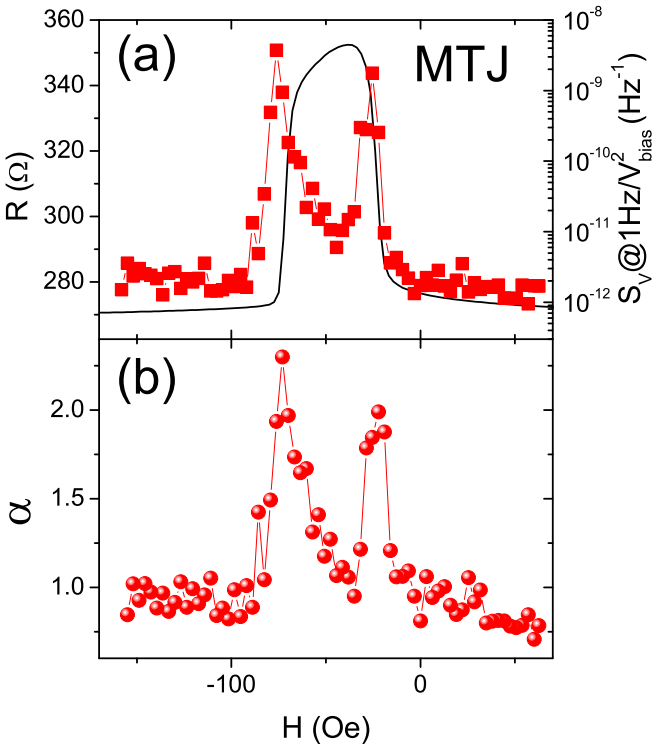

Figure 3 BP11179 28MAY2013

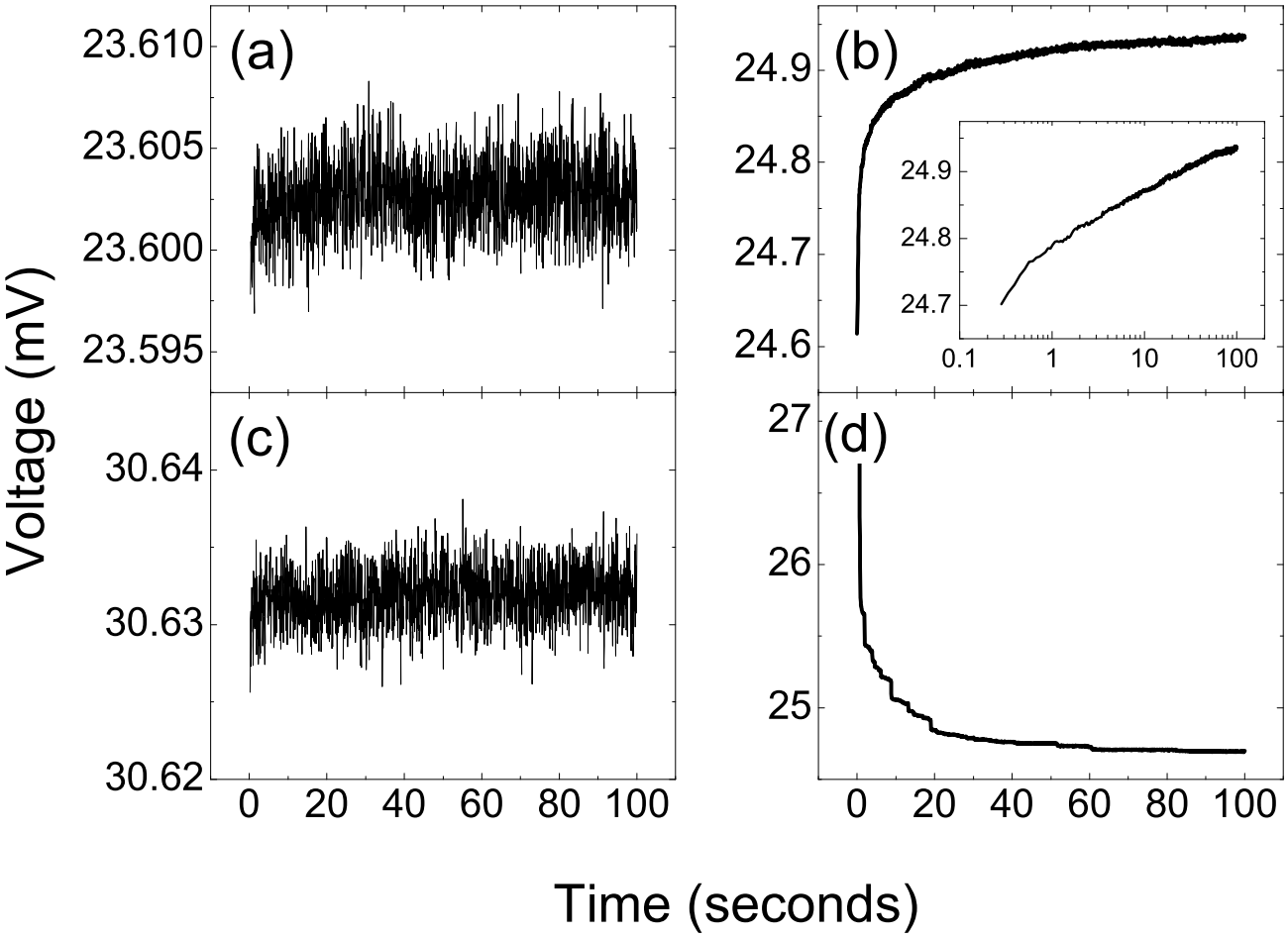

Figure 4 BP11179 28MAY2013

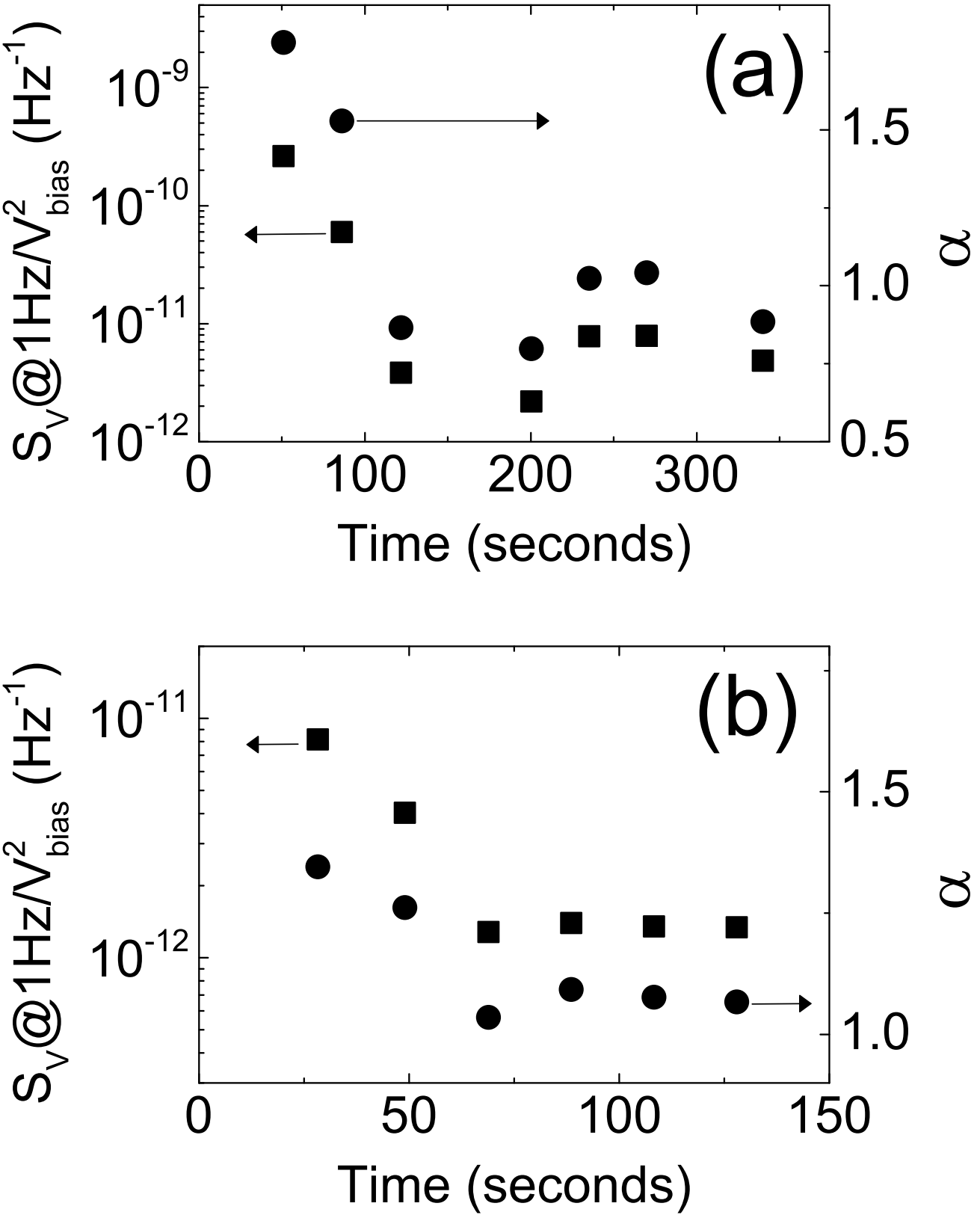

Figure 5 BP11179 28MAY2013

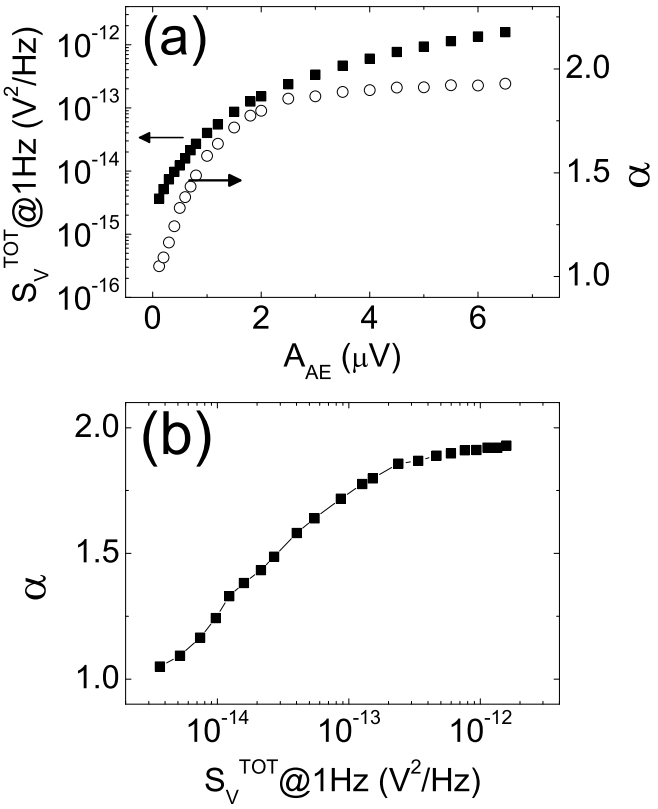

Figure 6 BP11179 28MAY2013

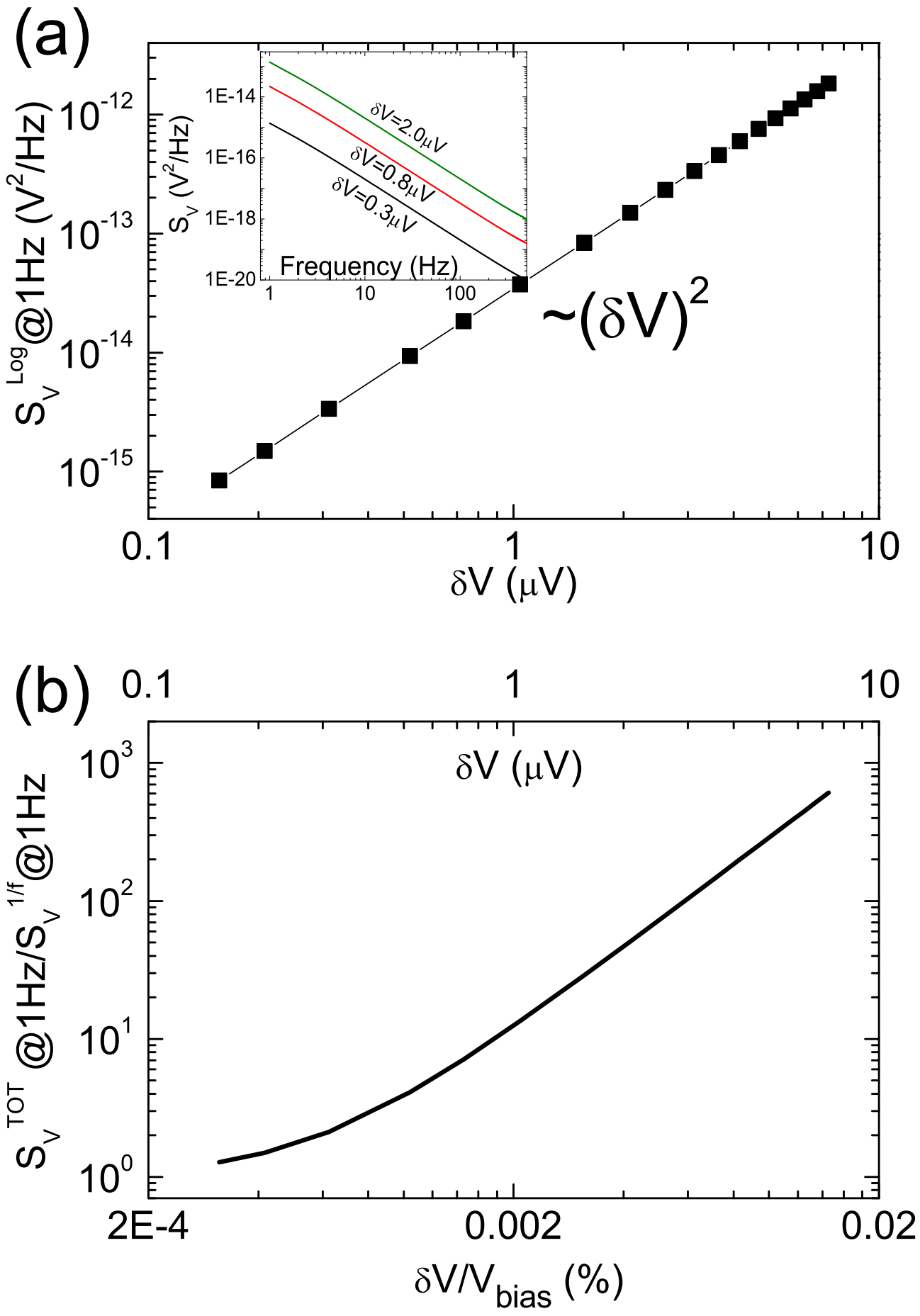

Figure 7 BP11179 28MAY2013

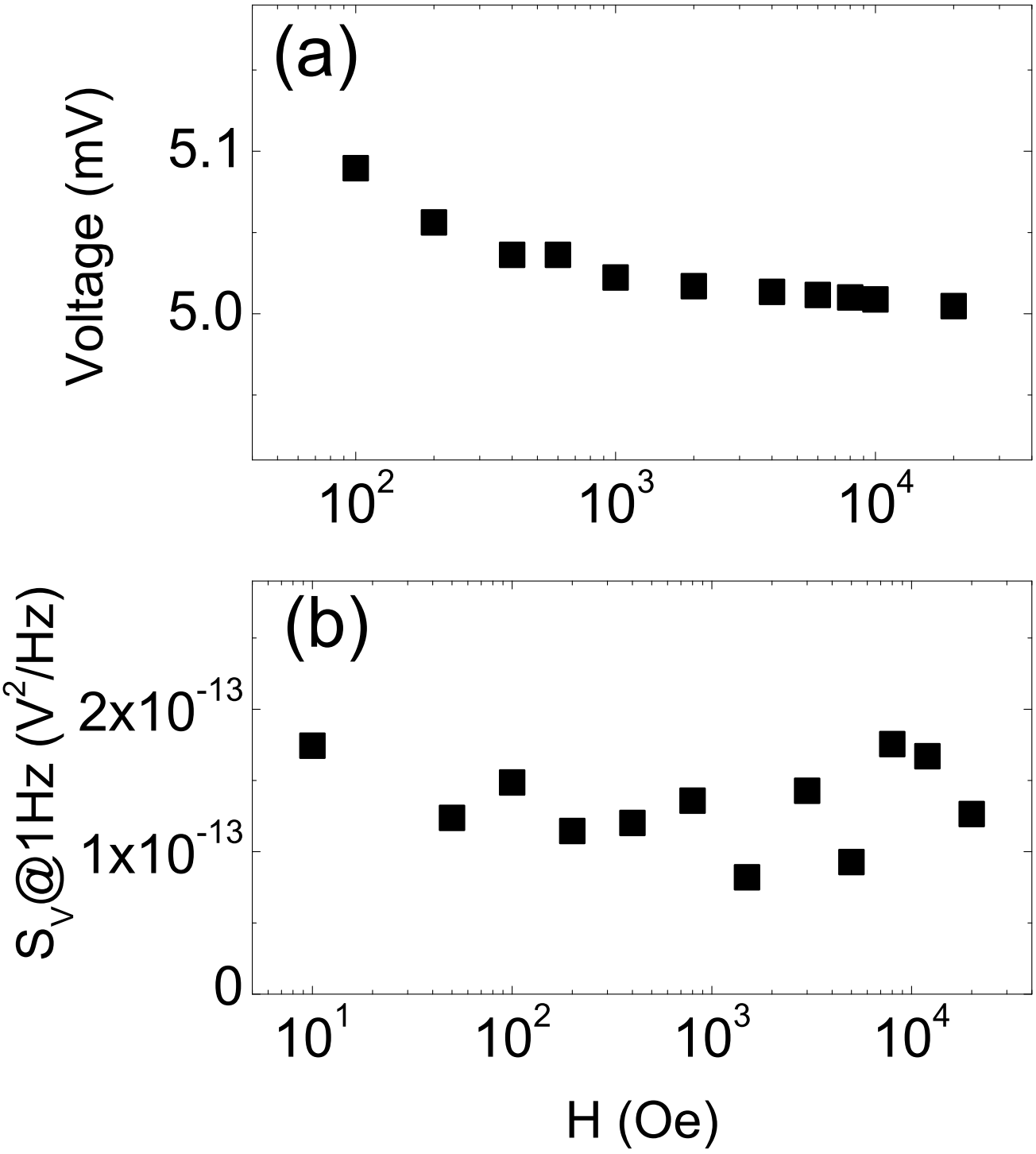

Figure 8 BP11179 28MAY2013

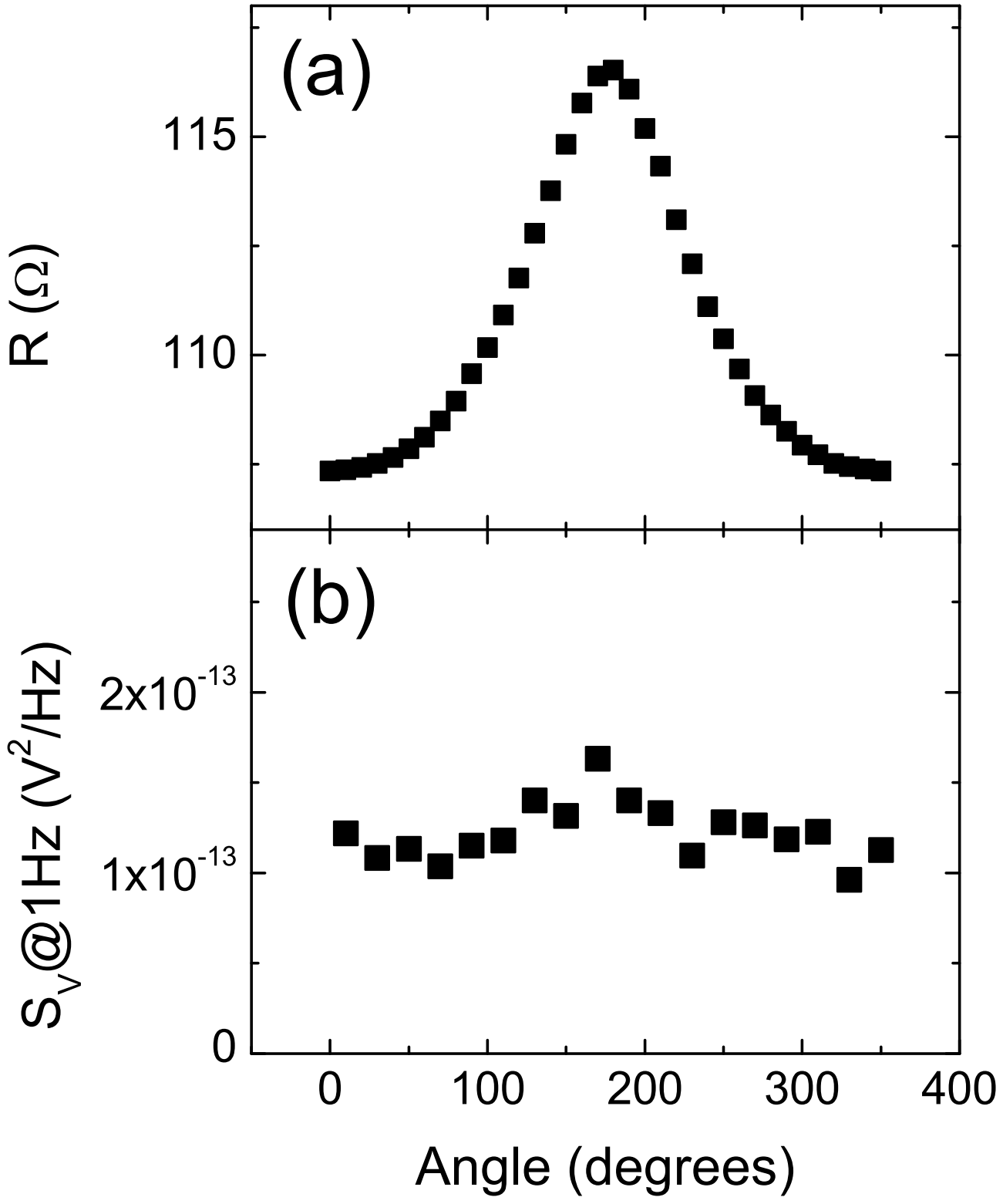

Figure 9 BP11179 28MAY2013